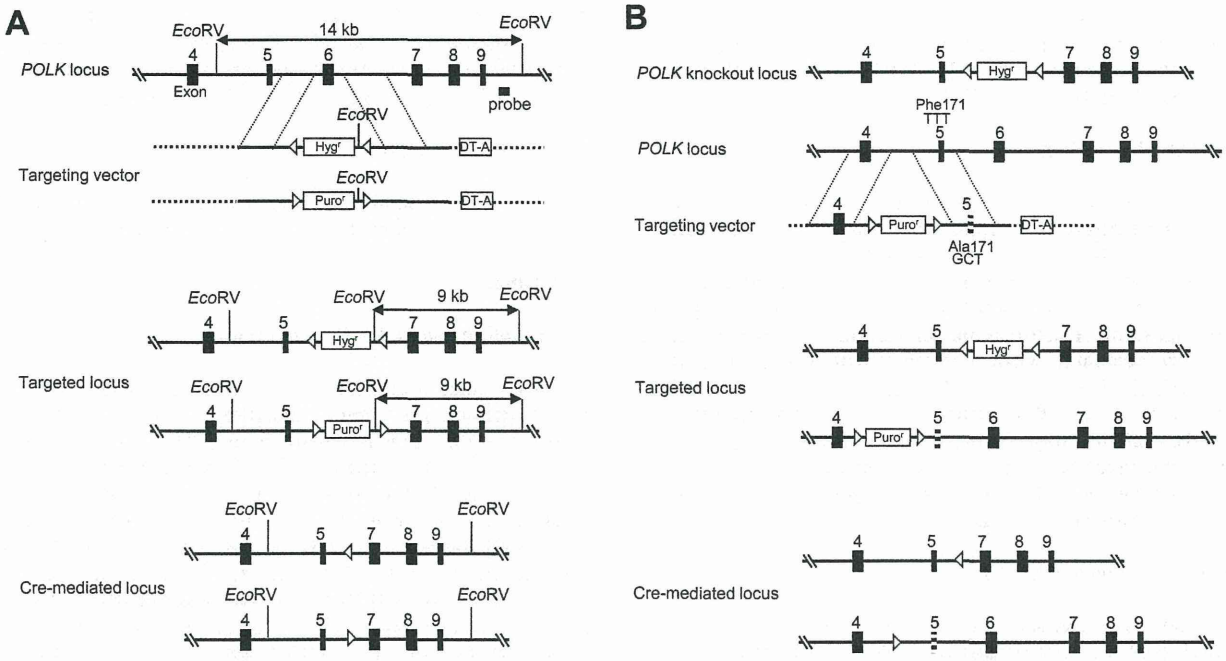

Fig. 1. Targeting strategy for generation of *POLK* mutant cells. Schematic representation of targeted disruption (A) and knock-in (B) of the *POLK* gene. The *POLK* locus, the targeting constructs, the targeted locus and the Cre-mediated locus are shown here. The black boxes, arrows and triangles represent exons, primers and *loxP* sequences, respectively. Phenylalanine 171 is coded in exon 5.

in the targeted alleles were removed by transient expression of Cre recombinase in the cells. The expression of Pol κ protein and mRNA in the established cells were confirmed by the Western blot analysis and RT-PCR (Fig. 2B and C). We confirmed no unintended mutations were introduced in exons 2, 3, 4 and 5 by DNA sequencing. The doubling time of $POLK^{F171A/-}$ (21.0 ± 0.71 h) and $POLK^{mock/-}$ (21.3 ± 0.49 h) cells were similar to that of $POLK^{+/-}$ cell as given above.

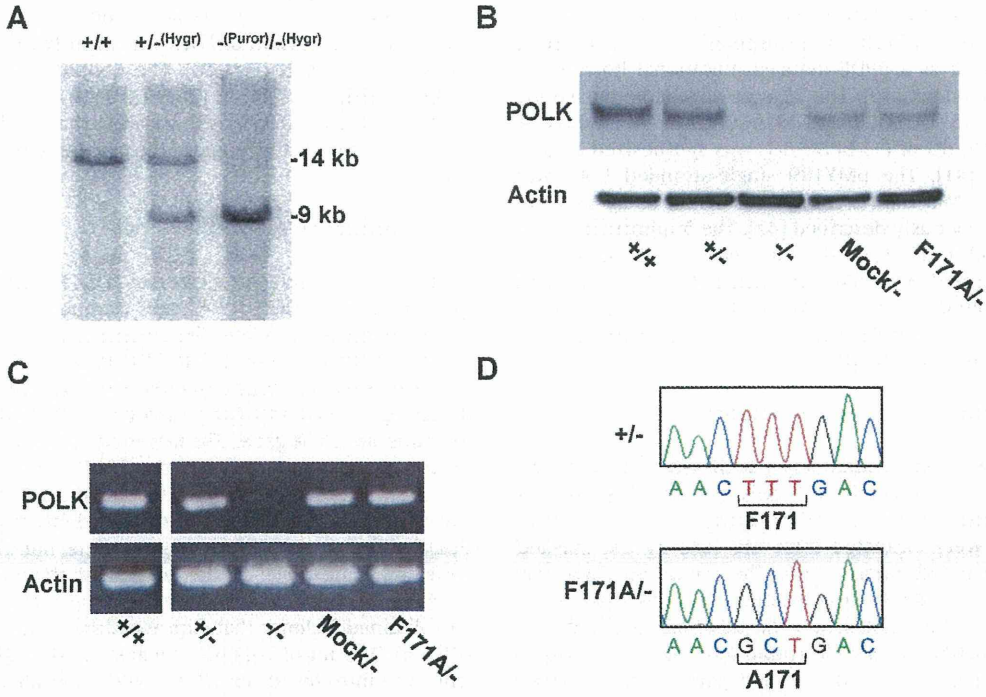

Fig. 2. Generation of $POLK^{+/-}$, $POLK^{-/-}$, and $POLK^{F171A/-}$ cells. (A) Southern blot analysis for *POLK* disruption. *Eco*RV-digested genomic DNA from wild-type (+/+), heterozygous (+/− (Hyg^r)), and homozygous (−(Puro^r)/−(Hyg^r)) *POLK* cells was loaded onto each lane. The probe used for the hybridization was indicated in Fig. 1. The wild-type allele (14 kb) and targeted alleles (9 kb) were indicated at right. (B) Western blot analysis for POLK protein. Whole cell extracts from $POLK^{+/+}$ $POLK^{+/-}$, $POLK^{-/-}$, $POLK^{mock/-}$, and $POLK^{F171A/-}$ cells were loaded onto a 10% of SDS-polyacrylamide gel. β-actin served as a loading control. (C) RT-PCR analysis for *POLK* mRNA. The same amounts of total RNA extracted from the each cell were used. β-actin served as an internal control. (D) Sequence of *POLK* cDNA generated by RT-PCR. The sequences around codon 171 were shown.

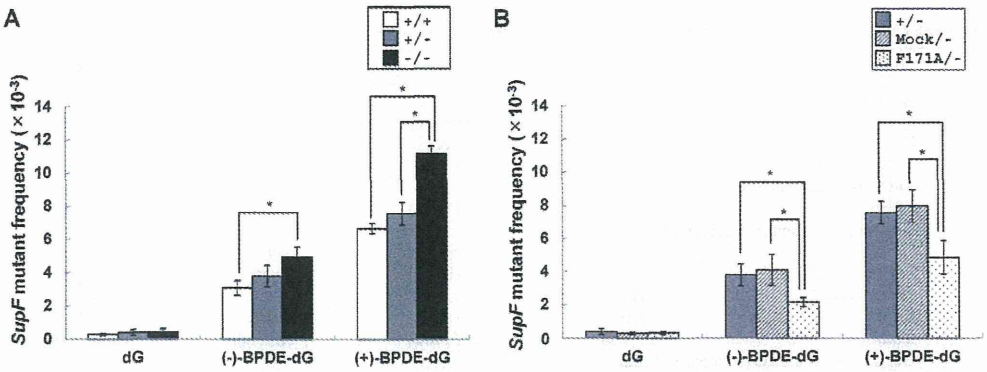

Fig. 3. Frequencies of the *supF* mutants induced by (−)- or (+)-*trans-anti*-BPDE-N^2-dG. Effect of (A) *POLK* disruption or (B) F171A knock-in on the mutant frequencies induced by dG:dC, (−)-*trans-anti*-BPDE-N^2-dG:dC, or (+)-*trans-anti*-BPDE-N^2-dG:dC pair. Data are expressed as mean ± standard deviation (SD) of 3 independent experiments. Asterisks indicate a significant difference with $P < 0.05$.

3.3. Effect of knock-out or knock-in of POLK on the mutant frequencies induced by BPDE-dG

Plasmid containing a single dG:dC, (−)-BPDE-dG:dC, or (+)-BPDE-dG:dC base-pair at position 123 of the *supF* gene was introduced and replicated in *POLK*$^{+/+}$, *POLK*$^{+/-}$, *POLK*$^{-/-}$, *POLK*$^{mock/-}$ or *POLK*$^{F171A/-}$ cells. Plasmids replicated in cells were recovered and introduced into the *E. coli* KS40/pOF105 indicator strain, in order to calculate the mutant frequencies for the *supF* gene [47].

We first examined the effect of the *POLK* knock-out on the mutagenesis induced by BPDE-dG adducts. As shown in Fig. 3A and Table S1, heterozygous and homozygous knock-out of *POLK* had no effect on the mutant frequency of the control plasmid containing dG:dC pair. In contrast, the mutant frequencies of the (−)-BPDE-dG:dC and (+)-BPDE-dG:dC pairs in *POLK*$^{+/-}$ cells (38×10^{-4} and 76×10^{-4}, respectively) were slightly higher than those in *POLK*$^{+/+}$ cells (31×10^{-4} and 67×10^{-4}, respectively), although the differences were not statistically significant. Furthermore, the mutant frequencies of these adducts were significantly increased in *POLK*$^{-/-}$ cells (49×10^{-4} and 112×10^{-4}, respectively) compared with those of *POLK*$^{+/+}$ cells, as consistent with the previous report [24].

Next, we examined the effect of the *POLK* F171A knock-in on the mutant frequencies of (−)- or (+)-BPDE-dG adducts in cells. Interestingly, the mutant frequencies of (−)-BPDE-dG:dC and (+)-BPDE-dG:dC pairs were significantly lower in *POLK*$^{F171A/-}$ cells (22×10^{-4} and 48×10^{-4}, respectively), as compared with *POLK*$^{+/-}$ (38×10^{-4} and 76×10^{-4}, respectively) and *POLK*$^{mock/-}$ cells (41×10^{-4} and 80×10^{-4}), respectively.

We further analyzed the mutation spectra induced by (−)-BPDE-dG:dC or (+)-BPDE-dG:dC pair in the *supF* gene in *POLK*$^{+/+}$, *POLK*$^{+/-}$, *POLK*$^{-/-}$, *POLK*$^{mock/-}$, or *POLK*$^{F171A/-}$ cells (Table 1). The most predominant mutation was G:C to T:A transversions at position 123 in all the cell lines. Lesser amount of G:C to C:G transversions, G:C to A:T transitions, one-base deletion, and tandem mutations at the adducted position were also observed. Neither knock-out of *POLK* nor knock-in of *POLK* F171A altered the mutation spectra induced by (−)-BPDE-dG:dC or (+)-BPDE-dG:dC.

4. Discussion

In the previous *in vitro* study, we revealed that F171A substitution of human Pol κ increases efficiency of dCMP incorporation opposite (−)- or (+)-BPDE-dG in DNA by 18 fold [35]. However, the k_{cat}/K_m values bypassing across the lesions by the wild-type Pol κ were 2–3 orders of magnitude smaller than those of incorporation of dCMP opposite normal dG. The small k_{cat}/K_m values for TLS across (−)- or (+)-BPDE-dG in DNA by the wild-type Pol κ have also been reported by other groups [19,23]. It was questioned, therefore, whether the increase in the k_{cat}/K_m value by the amino acid substitution *in vitro* has biological significance *in vivo*. To address the question, we established human cell lines expressing *POLK*$^{+/-}$, *POLK*$^{F171A/-}$, *POLK*$^{mock/-}$ and *POLK*$^{-/-}$ (KO) cells (Figs. 1 and 2) and examined the mutagenic sensitivities against plasmids carrying (−)- or (+)-BPDE-dG in the *supF* reporter gene. In the mutation assays, we employed a shuttle vector system, i.e., pMY189, to measure mutation frequencies induced by the specific DNA adduct although it is not very clear to what extent Pol κ behaves similarly in TLS in the plasmid and in the chromosome. (+)-BPDE-dG induced higher mutation frequencies than (−)-BPDE-dG regardless of the genotypes. These results are consistent with the previous results that (+)-BPDE-dG is more mutagenic than (−)-BPDE-dG [48,49]. Interestingly, the *POLK*$^{F171A/-}$ cells exhibited significantly lower frequencies of mutations induced by either (−)- or (+)-BPDE-dG compared to *POLK*$^{+/-}$ and *POLK*$^{mock/-}$ cells (Fig. 3). The spectrum of mutations induced by (−)- or (+)-BPDE-dG contained predominantly G:C to T:A at position 123 of the *supF* gene where the adducts were embedded regardless of the genotypes (Table 1). These results strongly suggest that the F171A derivative of Pol κ indeed continues DNA replication across (−)- and (+)-BPDE-dG in template DNA more efficiently than does the wild-type Pol κ in an error-free manner. It is formally possible that mutations are induced by the action of the F171A derivative of Pol κ because the derivative produces some errors during TLS across (−)- and (+)-BPDE-dG in template DNA *in vitro* [35]. However, we don't think this is the case because the derivative inserts dTMP in addition to dCMP opposite the adducts when one dNTP is present in the reaction mixture or induces one base deletions when four dNTPs are present in the mixture *in vitro*. These errors should lead to G:C to A:T transitions or one base deletions. As shown in Table 1, the predominant mutation observed in the cells expressing the F171A derivative was G:C to T:A transversions. In addition, the mutation spectra were not substantially different regardless of the status of Pol κ. Therefore, the mutations are generated by error-prone Pol(s) that inserts dAMP opposite the DNA adducts, not by the F171A derivative of Pol κ. Pol κ interacts with other proteins such as PCNA and REV1 *in vivo* [6]. These interactions may substantially enhance the efficiency of TLS by Pol κ, and thus the Pol may exhibit significant effects on TLS *in vivo* despite the small k_{cat}/K_m values *in vitro*.

Based on the current and previous results [35], along with the molecular dynamic studies [50] and the structure studies with the ternary complex of Pol κ [36], we conclude that F171 is a molecular brake for TLS across (−)- and (+)-BPDE-dG, in DNA by Pol κ. We speculate that F171 may flexibly rotate and interact with pyrene rings of both (−)- and (+)-BPDE-dG. Because F171A substitution

Table 1
Mutation spectra in *supF* induced by (−)- or (+)-*trans-anti*-BPDE-N^2-dG:dC in wild type, +/−, −/−, Mock/−, and F171A/− mutant cells.

Adduct[a]	Mutation	+/+	+/−	−/−	Mock/−	F171A/−
(−)-BPDE-dG	Single base substitution at site of adduct					
	^{123}G:C → T:A[b]	23 (62)[c]	47 (65)	45 (68)	24 (65)	22 (61)
	^{123}G:C → C:G	2 (5)	12 (17)	12 (18)	6 (16)	5 (14)
	^{123}G:C → A:T	7 (19)	11 (15)	6 (9)	7 (19)	9 (25)
	One base deletion at site of adduct					
	G^{123}GG → G-G[d]	0 (0)	1 (1)	0 (0)	0 (0)	0 (0)
	Tandem mutation at site of adduct					
	G^{123}GG → TTG	3 (8)	0 (0)	2 (3)	0 (0)	0 (0)
	G^{123}GG → −AG	2 (5)	0 (0)	0 (0)	0 (0)	0 (0)
	G^{123}GG → −TG	0 (0)	0 (0)	1 (2)	0 (0)	0 (0)
	Other	0 (0)	1 (1)	0 (0)	0 (0)	0 (0)
	Total	37 (100)	72 (100)	66 (100)	37 (100)	36 (100)
(+)-BPDE-dG	Single base substitution at site of adduct					
	^{123}G:C → T:A	34 (85)	66 (84)	59 (77)	33 (83)	30 (81)
	^{123}G:C → C:G	3 (8)	6 (8)	9 (12)	6 (15)	3 (8)
	^{123}G:C → A:T	1 (3)	5 (6)	2 (3)	0 (0)	2 (5)
	One base deletion at site of adduct					
	G^{123}GG → G-G	0 (0)	0 (0)	2 (3)	0 (0)	0 (0)
	Tandem mutation at site of adduct					
	G^{123}GG → TTG	2 (5)	1 (1)	3 (4)	1 (3)	1 (3)
	G^{123}GG → −TG	0 (0)	0 (0)	1 (1)	0 (0)	0 (0)
	G^{123}GG → GGGGGG	0 (0)	0 (0)	0 (0)	0 (0)	1 (3)
	Other	0 (0)	0 (0)	1 (1)	0 (0)	0 (0)
	Total	40 (100)	78 (100)	77 (100)	40 (100)	37 (100)

[a] (−)-BPDE-dG and (+)-BPDE-dG indicate (−)-*trans-anti*-BPDE-N^2-dG and (+)-*trans-anti*-BPDE-N^2-dG, respectively.
[b] ^{123}G indicates the position 123 in the *supF* gene.
[c] Numbers in parentheses represent the percentage of total number of mutants.
[d] "–" Indicates one-base deletion.

enhanced the error-free TLS across both lesions *in vitro* and *in vivo*, the interactions might interfere with correct Watson-Crick base-pairing between the modified dG and the incoming dCMP in the catalytic center of Pol κ. In general, the active sites of the Y-family Pols are more spacious than those of replicative Pols, allowing the accommodation of bulky adducts on the template bases [6]. The substitution of F171A could provide wider space in the active site, which enables Pol κ to more smoothly accommodate the lesion and continue DNA replication past the modified dG. In the previous study, we revealed that F171A substitution does not affect the fidelity of DNA replication across the lesions nor either the efficiency of dCMP incorporation opposite normal dG [35]. Thus, we suggest that the overall structure of Pol κ is not substantially affected by the amino acid substitution. There should be multiple Pols that compete with the primer DNA when replicative Pols are stalled at the lesions [6]. Due to the increased k_{cat}/K_m values incorporating dCMP opposite (−)- and (+)-BPDE-dG in DNA, the F171A derivative of Pol κ may become predominant over error-prone Pols, such as Pol ζ, thereby reducing the mutation frequencies. It is interesting that a variant form of TLS Pol has higher efficiency to continue DNA synthesis across the damage than the native form.

The conclusion that F171 is a molecular brake for DNA synthesis across BPDE adducts in DNA suggests that Pol κ is not well-tuned to bypass the adducts. Previous reports suggest that the cognate substrates for Pol κ may be BP adducts in DNA because the promoter region contains arylhydrocarbon receptor binding sites [51], and the mouse embryonic fibroblasts from *Polk*$^{-/-}$ mice exhibit hypersensitivity both to the killing effects of racemic-(±)-BPDE [34], and the mutagenic and lethal effects of BP plus rat liver homogenate (S9) in the presence of caffeine [33]. On the other hand, however, Pol κ binds only weakly to template/primer DNA containing (+)-BPDE adduct [25], which is the major DNA adduct induced by BPDE. Rather, it binds strongly to template/primer DNA containing (−)-BPDE adduct [25], which is a minor DNA adduct formed upon metabolic activation of BP. In addition, Pol κ more efficiently bypasses the (−)- adduct than the (+)-adduct [25]. These results along with the current *in vivo* results strongly suggest that Pol κ has not evolved to protect cells from BP or the related arylhydrocarbon carcinogens. This Pol is known to bypass other lesions induced by endogenous mutagens, i.e., methyl glyoxal [52], estrogen [53] and reactive oxygen species [54]. *Polk*$^{-/-}$ mice exhibit increased spontaneous mutations in the liver, kidney and lung, but not in testis, in older animals [34] and the mutation frequencies are enhanced by dietary cholesterol [55]. These results further suggest that the cognate lesion is the one induced by endogenous mutagens, which may increase the lesion in the organs during the aging process. These results may also explain why *POLK*$^{-/-}$ cells did not exhibit slow growth and high spontaneous mutation frequencies in this study. The cognate lesion might not be effectively induced in cultured cells.

In the current study, we took advantage of human Nalm-6 cells to engineer cell lines expressing a variant form of Pol κ. Unlike other human cell lines, which exhibit poor gene targeting efficiency, this cell line displays 1–30% gene targeting efficiencies [56]. In fact, we obtained one *POLK*$^{+/-}$ cell out of 132 wild-type cells (=0.8%) and one *POLK*$^{-/-}$ cell out of 158 *POLK*$^{+/-}$ cells (=0.6%). For the knock-in mutants, we obtained 2 *POLK*$^{F171A/-}$ cells out of 133 *POLK*$^{+/-}$ cells (=1.5%). Currently, gene knockdown with siRNA is the common technique to suppress gene expression in human cells because of the difficulty in obtaining such gene knock-out and knock-in cells. However, gene knockdown only reduces the expression by about 80% and does not completely shut it down. Embryonic fibroblasts from knock-out mice are an alternative available experimental resource by which to examine gene functions in mammals. Nevertheless, it is pointed out that the mouse cells do not exhibit similar TLS efficiency or accuracy compared to those of human cells [57]. Therefore, we believe that Nalm-6 cells are useful for genetic analyses of human genes including those involved in DNA repair and mutagenesis.

In summary, we established a human cell line expressing an F171 variant of Pol κ and suggest that this residue is used by Pol κ as a molecular brake for TLS across (−)- and (+)-BPDE-dG in DNA. The presence of such a brake in the active site raises a possibility that Pol κ has not evolved to protect cells from BP. Thus a complete

understanding of the role of Pol κ in protecting cells against the mutagenic and carcinogenic effects of endogenous mutagens is still lacking, and further investigations, both *in vitro* and *in vivo*, are needed.

Conflict of interest

We have no competing interests or conflicts of interest concerning the research presented in this paper.

Acknowledgments

This work was supported by grants-in-aid for scientific research from the Ministry of Education, Culture, Sports, Science and Technology, Japan (MEXT, 18201010; MEXT, 22241016), the Ministry of Health, Labour and Welfare, Japan (MHLW, H21-Food-General-009), and the Japan Health Science Foundation (KHB1007); for cancer research from MHLW (20 designated-8); the Food Safety Commission.

Appendix A. Supplementary data

Supplementary data associated with this article can be found, in the online version, at http://dx.doi.org/10.1016/j.dnarep.2013.12.008.

References

[1] E.C. Friedberg, R. Wagner, M. Radman, Specialized DNA polymerases, cellular survival, and the genesis of mutations, Science 296 (2002) 1627–1630.
[2] T. Nohmi, Environmental stress and lesion-bypass DNA polymerases, Annu. Rev. Microbiol. 60 (2006) 231–253.
[3] P.M. Burgers, E.V. Koonin, E. Bruford, L. Blanco, K.C. Burtis, M.F. Christman, W.C. Copeland, E.C. Friedberg, F. Hanaoka, D.C. Hinkle, C.W. Lawrence, M. Nakanishi, H. Ohmori, L. Prakash, S. Prakash, C.A. Reynaud, A. Sugino, T. Todo, Z. Wang, J.C. Weill, R. Woodgate, Eukaryotic DNA polymerases: proposal for a revised nomenclature, J. Biol. Chem. 276 (2001) 43487–43490.
[4] S. Prakash, R.E. Johnson, L. Prakash, Eukaryotic translesion synthesis DNA polymerases: specificity of structure and function, Annu. Rev. Biochem. 74 (2005) 317–353.
[5] S.S. Lange, K. Takata, R.D. Wood, DNA polymerases and cancer, Nat. Rev. Cancer 11 (2011) 96–110.
[6] J.E. Sale, A.R. Lehmann, R. Woodgate, Y-family DNA polymerases and their role in tolerance of cellular DNA damage, Nat. Rev. Mol. Cell Biol. 13 (2012) 141–152.
[7] C. Masutani, R. Kusumoto, A. Yamada, N. Dohmae, M. Yokoi, M. Yuasa, M. Araki, S. Iwai, K. Takio, F. Hanaoka, The *XPV* (xeroderma pigmentosum variant) gene encodes human DNA polymerase eta, Nature 399 (1999) 700–704.
[8] R.E. Johnson, C.M. Kondratick, S. Prakash, L. Prakash, hRAD30 mutations in the variant form of xeroderma pigmentosum, Science 285 (1999) 263–265.
[9] A.J. Rattray, J.N. Strathern, Error-prone DNA polymerases: when making a mistake is the only way to get ahead, Annu. Rev. Genet. 37 (2003) 31–66.
[10] K. Bebenek, T.A. Kunkel, Functions of DNA polymerases, Adv. Protein Chem. 69 (2004) 137–165.
[11] M.F. Goodman, Error-prone repair DNA polymerases in prokaryotes and eukaryotes, Annu. Rev. Biochem. 71 (2002) 17–50.
[12] H. Ling, F. Boudsocq, R. Woodgate, W. Yang, Snapshots of replication through an abasic lesion; structural basis for base substitutions and frameshifts, Mol. Cell 13 (2004) 751–762.
[13] V.L. Gerlach, W.J. Feaver, P.L. Fischhaber, E.C. Friedberg, Purification and characterization of pol kappa, a DNA polymerase encoded by the human *DINB1* gene, J. Biol. Chem. 276 (2001) 92–98.
[14] T. Ogi, T. Kato Jr., T. Kato, H. Ohmori, Mutation enhancement by DINB1, a mammalian homologue of the *Escherichia coli* mutagenesis protein *dinB*, Genes Cells 4 (1999) 607–618.
[15] R.E. Johnson, S. Prakash, L. Prakash, The human *DINB1* gene encodes the DNA polymerase Pol θ, Proc. Natl. Acad. Sci. U. S. A 97 (2000) 3838–3843.
[16] H. Ohmori, E.C. Friedberg, R.P. Fuchs, M.F. Goodman, F. Hanaoka, D. Hinkle, T.A. Kunkel, C.W. Lawrence, Z. Livneh, T. Nohmi, L. Prakash, S. Prakash, T. Todo, G.C. Walker, Z. Wang, R. Woodgate, The Y-family of DNA polymerases, Mol. Cell 8 (2001) 7–8.
[17] J. Wagner, P. Gruz, S.R. Kim, M. Yamada, K. Matsui, R.P. Fuchs, T. Nohmi, The *dinB* gene encodes a novel *E. coli* DNA polymerase, DNA pol IV, involved in mutagenesis, Mol. Cell 4 (1999) 281–286.
[18] P. Gruz, F.M. Pisani, M. Shimizu, M. Yamada, I. Hayashi, K. Morikawa, T. Nohmi, Synthetic activity of Sso DNA polymerase Y1, an archaeal DinB-like DNA polymerase, is stimulated by processivity factors proliferating cell nuclear antigen and replication factor C, J. Biol. Chem. 276 (2001) 47394–47401.
[19] N. Suzuki, E. Ohashi, A. Kolbanovskiy, N.E. Geacintov, A.P. Grollman, H. Ohmori, S. Shibutani, Translesion synthesis by human DNA polymeraseκ on a DNA template containing a single stereoisomer of dG-(+)- or dG-(-)-*anti*-N^2-BPDE (7 8-dihydroxy-anti-9,10-epoxy-7,8,9,10-tetrahydrobenzo[a]pyrene), Biochemistry 41 (2002) 6100–6106.
[20] Y. Zhang, F. Yuan, X. Wu, M. Wang, O. Rechkoblit, J.S. Taylor, N.E. Geacintov, Z. Wang, Error-free and error-prone lesion bypass by human DNA polymerase κ *in vitro*, Nucleic Acids Res. 28 (2000) 4138–4146.
[21] O. Rechkoblit, Y. Zhang, D. Guo, Z. Wang, S. Amin, J. Krzeminsky, N. Louneva, N.E. Geacintov, Translesion synthesis past bulky benzo[*a*]pyrene diol epoxide N^2-dG and N^6-dA lesions catalyzed by DNA bypass polymerases, J. Biol. Chem. 277 (2002) 30488–30494.
[22] J.Y. Choi, K.C. Angel, F.P. Guengerich, Translesion synthesis across bulky N^2-alkyl guanine DNA adducts by human DNA polymerase κ, J. Biol. Chem. 281 (2006) 21062–21072.
[23] X. Huang, A. Kolbanovskiy, X. Wu, Y. Zhang, Z. Wang, P. Zhuang, S. Amin, N.E. Geacintov, Effects of base sequence context on translesion synthesis past a bulky (+)-*trans-anti*-B[*a*]P-N^2-dG lesion catalyzed by the Y-family polymerase pol κ, Biochemistry 42 (2003) 2456–2466.
[24] S. Avkin, M. Goldsmith, S. Velasco-Miguel, N. Geacintov, E.C. Friedberg, Z. Livneh, Quantitative analysis of translesion DNA synthesis across a benzo[*a*]pyrene-guanine adduct in mammalian cells: the role of DNA polymerase kappa, J. Biol. Chem. 279 (2004) 53298–53305.
[25] N. Niimi, A. Sassa, A. Katafuchi, P. Gruz, H. Fujimoto, R.R. Bonala, F. Johnson, T. Ohta, T. Nohmi, The steric gate amino acid tyrosine 112 is required for efficient mismatched-primer extension by human DNA polymerase kappa, Biochemistry 48 (2009) 4239–4246.
[26] H. Fukuda, T. Takamura-Enya, Y. Masuda, T. Nohmi, C. Seki, K. Kamiya, T. Sugimura, C. Masutani, F. Hanaoka, H. Nakagama, Translesional DNA synthesis through a C8-guanyl adduct of 2-amino-1-methyl-6-phenylimidazo[4 5-b]pyridine (PhIP) in Vitro: Rev1 inserts dc opposite the lesion and DNA polymerase kappa potentially catalyzes extension reaction from the 3'-dC terminus, J. Biol. Chem. (2009).
[27] P.L. Fischhaber, V.L. Gerlach, W.J. Feaver, Z. Hatahet, S.S. Wallace, E.C. Friedberg, Human DNA polymerase κ bypasses and extends beyond thymine glycols during translesion synthesis *in vitro*, preferentially incorporating correct nucleotides, J. Biol. Chem. 277 (2002) 37604–37611.
[28] P. Jaloszynski, E. Ohashi, H. Ohmori, S. Nishimura, Error-prone and inefficient replication across 8-hydroxyguanine (8-oxoguanine) in human and mouse ras gene fragments by DNA polymerase kappa, Genes Cells 10 (2005) 543–550.
[29] I.G. Minko, M.B. Harbut, I.D. Kozekov, A. Kozekova, P.M. Jakobs, S.B. Olson, R.E. Moses, T.M. Harris, C.J. Rizzo, R.S. Lloyd, Role for DNA polymerase kappa in the processing of N^2-N^2-guanine interstrand cross-links, J. Biol. Chem. 283 (2008) 17075–17082.
[30] D.H. Phillips, P.L. Grover, Polycyclic hydrocarbon activation: bay regions and beyond, Drug Metab. Rev. 26 (1994) 443–467.
[31] K. Peltonen, A. Dipple, Polycyclic aromatic hydrocarbons: chemistry of DNA adduct formation, J. Occup. Environ. Med. 37 (1995) 52–58.
[32] Y. Zhang, X. Wu, D. Guo, O. Rechkoblit, N.E. Geacintov, Z. Wang, Two-step error-prone bypass of the (+)- and (-)-*trans-anti*-BPDE-N^2-dG adducts by human DNA polymerases eta and kappa, Mutat. Res. 510 (2002) 23–35.
[33] T. Ogi, Y. Shinkai, K. Tanaka, H. Ohmori, Polκ protects mammalian cells against the lethal and mutagenic effects of benzo[*a*]pyrene, Proc. Natl. Acad. Sci. U. S. A 99 (2002) 15548–15553.
[34] J.N. Stancel, L.D. McDaniel, S. Velasco, J. Richardson, C. Guo, E.C. Friedberg, *Polk* mutant mice have a spontaneous mutator phenotype, DNA Rep. (Amst) 8 (2009) 1355–1362.
[35] A. Sassa, N. Niimi, H. Fujimoto, A. Katafuchi, P. Gruz, M. Yasui, R.C. Gupta, F. Johnson, T. Ohta, T. Nohmi, Phenylalanine 171 is a molecular brake for translesion synthesis across benzo[*a*]pyrene-guanine adducts by human DNA polymerase kappa, Mutat. Res. 718 (2011) 10–17.
[36] S. Lone, S.A. Townson, S.N. Uljon, R.E. Johnson, A. Brahma, D.T. Nair, S. Prakash, L. Prakash, A.K. Aggarwal, Human DNA polymerase κ encircles DNA: implications for mismatch extension and lesion bypass, Mol. Cell 25 (2007) 601–614.
[37] T. Suzuki, A. Ukai, M. Honma, N. Adachi, T. Nohmi, Restoration of mismatch repair functions in human cell line Nalm-6, which has high efficiency for gene targeting, PLoS One 8 (2013) e61189.
[38] S. Iiizumi, Y. Nomura, S. So, K. Uegaki, K. Aoki, K. Shibahara, N. Adachi, H. Koyama, Simple one-week method to construct gene-targeting vectors: application to production of human knockout cell lines, Biotechniques 41 (2006) 311–316.
[39] S. So, N. Adachi, M.R. Lieber, H. Koyama, Genetic interactions between BLM and DNA ligase IV in human cells, J. Biol. Chem. 279 (2004) 55433–55442.
[40] J.L. Yang, V.M. Maher, J.J. McCormick, Kinds of mutations formed when a shuttle vector containing adducts of (+/-)-7β 8α-dihydroxy-9α, 10α-epoxy-7,8,9, 10-tetrahydrobenzo[a]pyrene replicates in human cells, Proc. Natl. Acad. Sci. U. S. A 84 (1987) 3787–3791.
[41] F. Johnson, R. Bonala, D. Tawde, M.C. Torres, C.R. Iden, Efficient synthesis of the benzo[*a*]pyrene metabolic adducts of 2′-deoxyguanosine and 2′-deoxyadenosine and their direct incorporation into DNA, Chem. Res. Toxicol. 15 (2002) 1489–1494.
[42] H. Kamiya, H. Kasai, 2-Hydroxy-dATP is incorporated opposite G by Escherichia coli DNA polymerase III resulting in high mutagenicity, Nucleic Acids Res. 28 (2000) 1640–1646.

[43] N. Sunaga, T. Kohno, K. Shinmura, T. Saitoh, T. Matsuda, R. Saito, J. Yokota, OGG1 protein suppresses G:C → T:A mutation in a shuttle vector containing 8-hydroxyguanine in human cells, Carcinogenesis 22 (2001) 1355–1362.
[44] A. Stary, A. Sarasin, Simian virus 40 (SV40) large T antigen-dependent amplification of an Epstein-Barr virus-SV40 hybrid shuttle vector integrated into the human HeLa cell genome, J. Gen. Virol. 73 (Pt 7) (1992) 1679–1685.
[45] F. Obata, T. Nunoshiba, T. Hashimoto-Gotoh, K. Yamamoto, An improved system for selection of forward mutations in an *Escherichia coli supF* gene carried by plasmids, J. Radiat. Res. 39 (1998) 263–270.
[46] N. Murata-Kamiya, H. Kamiya, H. Kaji, H. Kasai, Glyoxal, a major product of DNA oxidation, induces mutations at G:C sites on a shuttle vector plasmid replicated in mammalian cells, Nucleic Acids Res. 25 (1997) 1897–1902.
[47] T. Yagi, The achievement of shuttle vector techniques in mammalian mutation research, Genes Environ. 35 (2013) 93–98.
[48] M. Moriya, S. Spiegel, A. Fernandes, S. Amin, T. Liu, N. Geacintov, A.P. Grollman, Fidelity of translesional synthesis past benzo[a]pyrene diol epoxide-2′-deoxyguanosine DNA adducts: marked effects of host cell, sequence context, and chirality, Biochemistry 35 (1996) 16646–16651.
[49] P. Brookes, M.R. Osborne, Mutation in mammalian cells by stereoisomers of anti-benzo[a]pyrene-diolepoxide in relation to the extent and nature of the DNA reaction products, Carcinogenesis 3 (1982) 1223–1226.
[50] L. Jia, N.E. Geacintov, S. Broyde, The N-clasp of human DNA polymerase kappa promotes blockage or error-free bypass of adenine- or guanine-benzo[a]pyrenyl lesions, Nucleic Acids Res. 36 (2008) 6571–6584.
[51] T. Ogi, J. Mimura, M. Hikida, H. Fujimoto, Y. Fujii-Kuriyama, H. Ohmori, Expression of human and mouse genes encoding polκ: testis-specific developmental regulation and AhR-dependent inducible transcription, Genes Cells 6 (2001) 943–953.
[52] B. Yuan, C. You, N. Andersen, Y. Jiang, M. Moriya, T.R. O'Connor, Y. Wang, The roles of DNA polymerases kappa and iota in the error-free bypass of N2-carboxyalkyl-2′-deoxyguanosine lesions in mammalian cells, J. Biol. Chem. 286 (2011) 17503–17511.
[53] A. Mizutani, T. Okada, S. Shibutani, E. Sonoda, H. Hochegger, C. Nishigori, Y. Miyachi, S. Takeda, M. Yamazoe, Extensive chromosomal breaks are induced by tamoxifen and estrogen in DNA repair-deficient cells, Cancer Res. 64 (2004) 3144–3147.
[54] J.H. Yoon, G. Bhatia, S. Prakash, L. Prakash, Error-free replicative bypass of thymine glycol by the combined action of DNA polymerases kappa and zeta in human cells, Proc. Natl. Acad. Sci. U. S. A 107 (2010) 14112–14116.
[55] W.D. Singer, L.C. Osimiri, E.C. Friedberg, Increased dietary cholesterol promotes enhanced mutagenesis in DNA polymerase kappa-deficient mice, DNA Rep. (Amst) 12 (2013) 817–823.
[56] N. Adachi, S. So, S. Iiizumi, Y. Nomura, K. Murai, C. Yamakawa, K. Miyagawa, H. Koyama, The human pre-B cell line Nalm-6 is highly proficient in gene targeting by homologous recombination, DNA Cell Biol. 25 (2006) 19–24.
[57] S. Shachar, O. Ziv, S. Avkin, S. Adar, J. Wittschieben, T. Reissner, S. Chaney, E.C. Friedberg, Z. Wang, T. Carell, N. Geacintov, Z. Livneh, Two-polymerase mechanisms dictate error-free and error-prone translesion DNA synthesis in mammals, EMBO J. 28 (2009) 383–393.

IVYSPRING INTERNATIONAL PUBLISHER

International Journal of Biological Sciences

2014; 10(1):73-79. doi: 10.7150/ijbs.5750

Research Paper

Mismatch Repair Deficient Mice Show Susceptibility to Oxidative Stress-Induced Intestinal Carcinogenesis

Jingshu Piao[1], Yoshimichi Nakatsu[1], Mizuki Ohno[1], Ken-ichi Taguchi[2], Teruhisa Tsuzuki[1] ✉

1. Department of Medical Biophysics and Radiation Biology, Graduate School of Medical Sciences, Kyushu University,
2. Department of Cancer Pathology, Institute for Clinical Research, National Kyushu Cancer Center, Fukuoka, Japan

✉ Corresponding author: Teruhisa Tsuzuki, Department of Medical Biophysics and Radiation Biology, Faculty of Medical Sciences, Kyushu University, Fukuoka 812-8582, Japan. Phone: +81-92-642-6141: fax: +81-92-642-6145: E-mail: tsuzuki@med.kyushu-u.ac.jp

Received: 2012.12.21; Accepted: 2013.07.24; Published: 2013.12.19

Abstract

We have previously established an experimental system for oxidative DNA damage-induced tumorigenesis in the small intestine of mice. To elucidate the roles of mismatch repair genes in the tumor suppression, we performed oxidative DNA damage-induced tumorigenesis experiments using *Msh2*-deficient mice. Oral administration of 0.2% Potassium Bromate, $KBrO_3$, effectively induced epithelial tumors in the small intestines of *Msh2*-deficient mice. We observed a 22.5-fold increase in tumor formation in the small intestines of *Msh2*-deficient mice compared with the wild type mice. These results indicate that mismatch repair is involved in the suppression of oxidative stress-induced intestinal tumorigenesis in mice. A mutation analysis of the *Ctnnb1* gene of the tumors revealed predominant occurrences of G:C to A:T transitions. The TUNEL analysis showed a decreased number of TUNEL-positive cells in the crypts of small intestines from the *Msh2*-deficient mice compared with the wild type mice after treatment of $KBrO_3$. These results suggest that the mismatch repair system may simultaneously function in both avoiding mutagenesis and inducing cell death to suppress the tumorigenesis induced by oxidative stress in the small intestine of mice.

Key words: HNPCC, oxidative DNA damage, Wnt signaling pathway, mutagenesis, cell death

Introduction

Reactive oxygen species (ROS) are generated by the normal cellular metabolism and also by exposure to environmental factors, such as radiation and chemicals. ROS constantly induce various lesions in the DNA of living organisms under physiological conditions, and the resulting DNA damage causes mutations and cell death, leading to aging-associated diseases, such as cancer and neurodegeneration (1). Among the various types of oxidative DNA damage, oxidized guanine, 8-oxo-7, 8-dihydroguanine (8-oxoG) is abundant and highly mutagenic because of its ambiguous base-pairing properties; it can be paired with adenine as well as with cytosine (2-6). Therefore, 8-oxoG in DNA causes G:C to T:A transversions after two rounds of DNA replication. In mammalian cells, the base excision repair (BER) pathway initiated by OGG1 or MUTYH plays a role in the suppression of 8-oxoG-related mutagenesis. OGG1, an 8-oxoG DNA glycosylase, excises the 8-oxoG paired with cytosine from DNA (7, 8). MUTYH is an adenine DNA glycosylase that excises the adenine incorporated opposite 8-oxoG from DNA (9-12). The synergistic actions of OGG1 and MUTYH suppress the mutagenesis caused by 8-oxoG in DNA.

In addition to DNA repair, a nucleotide pool sanitizing enzyme, MTH1, suppresses the mutagenesis induced by oxidative stress (13, 14). This enzyme can hydrolyze oxidized purine nucleotides, such as 8-oxo-dGTP, 2-OH-dATP and 8-OH-dATP, to prevent the incorporation of mutagenic nucleotides into DNA

during replication (15, 16). In addition to 8-oxoG, a wide variety of oxidatively modified bases in DNA were removed by the BER pathway following initiation by various DNA glycosylases (17).

Besides BER, mismatch repair (MMR) is also involved in the repair of oxidative DNA damage. MMR is an evolutionarily conserved system that corrects replication errors such as mismatched bases and small insertions/deletions. The MSH2/MSH6 heterodimer (MutSα) and MSH2/MSH3 heterodimer (MutSβ) recognize mismatched bases and small insertions/deletions, respectively, and then recruit MutLα (MLH1 and PMS2 heterodimer) to initiate the MMR reaction (18). In addition to its role in correcting replication errors, MMR is known to involve in the induction of apoptosis in response to DNA lesions caused by alkylating agents (19-21). The human MMR genes are associated with hereditary non-polyposis colorectal cancer (HNPCC), which is a common cancer predisposition syndrome characterized by a dominant mode of transmission and high penetrance (22-25). deWeese *et al* reported that *Msh2*-deficient mouse embryonic stem (ES) cells showed the accumulation of oxidative DNA damage, such as 8-oxoG and thymine glycol, in their genomes, as well as tolerance to apoptosis caused by low dose gamma-ray irradiation (26). Based on the analysis of spontaneous mutational specificity of mice defective in the *Mth1* and/or the *Msh2* genes, we speculated that MMR might act to correct mispairs with the oxidized nucleotides (27). Furthermore, Colussi *et al*, and Russo *et al* reported that MMR could suppress the mutations caused by the incorporation of oxidized purine deoxynucleoside triphosphate (28, 29). These findings suggest the involvement of MMR in the suppression of oxidative stress-induced mutagenesis and tumorigenesis in mammals.

$KBrO_3$ is an oxidizing agent that is known to induce 8-oxoG in the DNA of rats and mice, and is recognized as a renal carcinogen in rats (30-33). We previously established an experimental system for oxidative DNA damage-induced tumorigenesis in the intestinal tract of mice using this agent (34). The oral administration of $KBrO_3$ for 16 weeks effectively induced epithelial tumors in the small intestines of *Mutyh*-deficient mice, indicating the significance of Mutyh in the suppression of tumorigenesis induced by oxidative stress (34).

In this study, we performed $KBrO_3$-induced tumorigenesis experiments using *Msh2*-deficient mice to elucidate the roles of MMR in the suppression of oxidative stress-induced tumorigenesis. We found that MMR plays a significant role in the suppression of oxidative stress-induced intestinal tumorigenesis in mice.

Materials and Methods

Animals

The *Msh2*-deficient mice used in this study were generated as reported previously (27). The wild type, heterozygous and homozygous mutant mice used in this study were obtained by intercrossing the heterozygous mutant mice. All animals were maintained under specific pathogen free (SPF) conditions. All animal care and handling procedures were approved by the Institutional Animal Care and Use Committee of Kyushu University, and followed the Guideline for Proper Conduct of Animal Experiments, Science Council of Japan.

$KBrO_3$ treatment

$KBrO_3$ (Sigma-ALDRICH) was given to 6~8-week-old mice in their drinking water at a concentration of 0.2% for 16 weeks. The body weight and consumption of drinking water were measured every week. After 16 weeks, all the animals were sacrificed, and the intestines were fixed with 10% phosphate buffered-formalin, and then stored in 70% ethanol.

Histological analysis

The inspections for tumor formation in the intestinal mucosa were carefully performed under a dissecting microscope. The small intestinal tumors were carefully removed from intestines, embedded in paraffin and sectioned. The sections were stained with hematoxylin and eosin for the diagnosis of the tumors. The evaluation of the tumors was performed according to the Vienna classification (35).

Mutation analysis of the *Ctnnb1* gene

The small intestinal tumors were carefully removed from the mucosa under a dissecting microscope. Genomic DNA was extracted using a DNeasy Tissue Kit (QIAGEN) according to the manufacturer's protocol. Eighty-nine small intestinal tumors obtained from five *Msh2*-deficient mice were analyzed for mutations in the *Ctnnb1* (*β-catenin*) gene. Thirty to fifty nanograms of genomic DNA extracted from each small intestinal tumor was used as the template for PCR with rTaq DNA polymerase (TaKaRa). The entire coding sequence of the second exon of the *Ctnnb1* gene was amplified using primers 5′-TCCTTGGCTGCCTTTCTAACAGTA-3′ (upper) and 5′-GCATGCCCTCATCTAGCGTCT-3′ (lower). Amplified DNA containing exon 2 of the *Ctnnb1* gene was purified with a PCR purification kit (QIAGEN) according to the manufacturer's protocol. The purified DNA fragments were used as a template for direct sequencing with a BigDye Terminator v3.1 Cycle Sequencing kit (Applied Biosystems) and the se-

quences were determined with an ABI PRISM® 3100 Genetic Analyzer (Applied Biosystems).

TUNEL analysis

The intestines were removed from the wild type and mutant mice treated with $KBrO_3$ for 16 weeks, and 3 μm sections were made after the samples were embedded in paraffin. We analyzed the cell death (apoptosis) in the crypts of the small intestine using a TUNEL kit (TaKaRa) as described in the manual supplied by the manufacturer. We counted the TUNEL-positive cells in more than 100 crypts from five mice of each genotype.

Results

Tumor formation induced by $KBrO_3$ treatment in *Msh2*-deficient mice

In order to examine whether oxidative stress increases the intestinal tumorigenesis in mismatch repair-deficient mice, congenic wild type, heterozygous and homozygous *Msh2*-deficient (5, 6 and 7 animals for each genotype, respectively) mice were administered 0.2% $KBrO_3$ in their drinking water for 16 weeks. At the same time, five mice of each genotype were kept under the same conditions except for the $KBrO_3$-treatment. As previously observed, the $KBrO_3$-treatment appeared to cause a slowdown in the increase of body weight at almost the same rate in all groups of animals during the period of $KBrO_3$-treatment. We dissected the mice after the 16-week treatment with $KBrO_3$, and inspected the intestines under a dissecting microscope. In the homozygous *Msh2*-deficient mice treated with $KBrO_3$, the formation of small intestinal tumors was dramatically increased (Figure 1, Table 1). The mean number of tumors induced in the small intestines of the seven *Msh2*-deficient mice was 27.0, whereas it was 1.2 and 1.5 in the five wild type and six heterozygous mice, respectively. Tumor formation was also observed in the untreated homozygous *Msh2*-deficient mice, albeit at a much lower frequency (mean: 1.2 tumor/mouse, n=5) compared with the treated homozygous mice. As previously observed in the *Mutyh*-deficient mice (34), the $KBrO_3$-induced tumors predominantly developed in the duodenum and in the upper region of the jejunum (Figure 1A). We found no other anomalies in the $KBrO_3$-treatment mice.

Table 1. Tumor formation in the intestine of *Msh2*-deficient mice

Genotype	No treatment	$KBrO_3$-treatment	
	No. of tumors[a]	No. of tumors[a]	Ratio[b]
Wild type	0	1.20 ± 0.98	1.00
Heterozygote	0	1.50 ± 1.26	1.25
Homozygote	1.20 ± 0.75	27.00 ± 7.44	22.50

a: The no. of tumors is the mean number of tumors per mouse, with the standard deviation. b: ratio to tumors in wild type mice

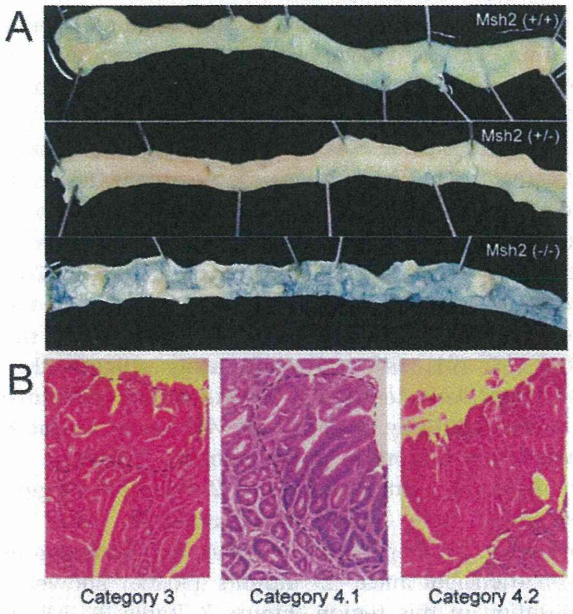

Figure 1. $KBrO_3$-induced tumors in the small intestine of *Msh2*-deficient mice. *A.* The proximal regions of the small intestines of $KBrO_3$-treated mice are shown; (+/+): wild type, (+/-): heterozygous *Msh2*-deficient, and (-/-): homozygous *Msh2*-deficient mice. Multiple polyp formations could be observed in the $KBrO_3$-treated homozygous *Msh2*-deficient mice. ***B.*** A section of a $KBrO_3$-induced tumor stained with hematoxylin and eosin (original magnification: objective 10X). The regions containing the neoplasia are encircled by a broken line.

Pathological analysis of tumors induced by $KBrO_3$ in the small intestines

We performed a pathological analysis of 25, three and two small intestinal tumors derived from five homozygous-deficient, three heterozygous *Msh2*-deficient mice and two wild type mice, respectively, according to the Vienna classification of gastrointestinal epithelial neoplasia (Table 2, Figure 1B). All tumors from homozygous *Msh2*-deficient mice were classified as category 4 (non-invasive high grade neoplasia), except for one case that was classified as category 3 (non-invasive low grade neoplasia). All tumors from wild type and heterozygous *Msh2*-deficient mice were also classified as category 4 (Table 2).

Table 2. Classification of $KBrO_3$-induced small intestinal tumors in mice

Genotype	Category 3*	Category 4*			Total
		4.1	4.2	4.3	
Wild type	—	—	2	—	2
Heterozygote	—	—	3	—	3
Homozygote	1	3	21	—	25

*Tumors were categorized according to the Vienna classification of gastrointestinal epithelial neoplasia

Mutation analysis of the *Ctnnb1* gene

The β-catenin protein encoded by *Ctnnb1* gene is a transcriptional activator functioning in the Wnt-signaling pathway (36). The phosphorylation of β-catenin by GSK3β in a complex with Axin and Apc is required for the ubiquitin-mediated degradation of β-catenin. Therefore, the presence of mutations affecting the phosphorylation of the protein lead to its stabilization and the accumulation of β-catenin in nuclei, inducing the expression of target genes such as c-myc and cyclin D1 without Wnt signaling. The mutations at four putative GSK3β-phosphorylation sites (S33, S37, T41, S45) and amino acids adjacent these sites have been detected in a wide variety of human cancers including HNPCC, as well as in chemically-induced tumors in model animals. Therefore, we analyzed the mutations in exon 2 of the *Ctnnb1* gene encoding the GSK3β-phosphorylation sites of β-catenin. Among 89 tumors from five homozygous *Msh2*-deficient mice, 27 tumors (30.3%) showed a mutation in this region (Figure 2, Table 3). All the mutations were base substitutions and occurred at or in the vicinity of the codons for S33, S37 and T41. No mutations were observed at the codon for S45. Among them, G:C to A:T transitions predominantly occurred; 20 mutations (74.1%) were identified as G:C to A:T transitions, and the others were three A:T to G:C transitions (11.1%), two G:C to T:A transversions and two G:C to C:G transversions (7.4%, respectively). There is no clear hotspot for G:C to A:T transitions in this region, with there being seven at D32, five at S37, four at G34 and four at T41. However, besides one G:C to T:A transversion at S33, three other types of mutations were observed only at the codon for S37. The base substitutions observed at the codon for S37 were as follows; five G:C to A:T transitions, three A:T to G:C transitions, two G:C to C:G transversions and one G:C to T:A transversion.

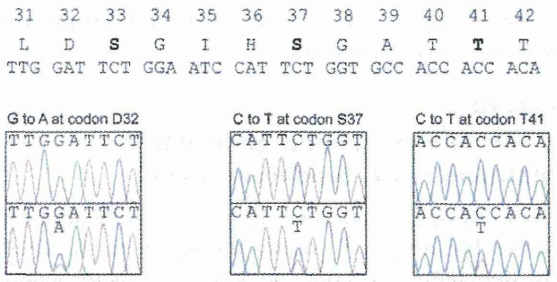

Figure 2. Somatic mutations found in the *Ctnnb1* gene of tumors. The amino acid sequence and the corresponding nucleotide sequence of GSK3β phosphorylation sites are shown at the top. The amino acids at phosphorylation sites are depicted in bold. The somatic mutations found in the $KBrO_3$-induced intestinal tumors are shown below the nucleotide sequence of the *Ctnnb1* gene; upper and lower panels show the nucleotide sequencing results from normal tissues and tumors, respectively.

Table 3. Mutations found in the *Ctnnb1* gene

Mouse ID	Sample ID	Nucleotide position	Wild type	Mutant	Mutation	Amino acid change
22	1	94	GAT	AAT	G:C→A:T	D32N
38	1	109	TCT	CCT	A:T→G:C	S37P
	4	109	TCT	CCT	A:T→G:C	S37P
	5	122	ACC	ATC	G:C→A:T	T41I
	7	101	GGA	GAA	G:C→A:T	G34E
	8	110	TCT	TAT	G:C→T:A	S37Y
	12	94	GAT	AAT	G:C→A:T	D32N
	13	100	GGA	AGA	G:C→A:T	G34R
	18	110	TCT	TTT	G:C→A:T	S37F
	20	110	TCT	TTT	G:C→A:T	S37F
	21	122	ACC	ATC	G:C→A:T	T41I
	22	94	GAT	AAT	G:C→A:T	D32N
48	4	110	TCT	TGT	G:C→C:G	S37C
	6	110	TCT	TTT	G:C→A:T	S37F
	10	94	GAT	AAT	G:C→A:T	D32N
	15	100	GGA	AGA	G:C→A:T	G34R
	22	109	TCT	CCT	A:T→G:C	S37P
45	1	122	ACC	ATC	G:C→A:T	T41I
	3	110	TCT	TGT	G:C→C:G	S37C
	9	110	TCT	TTT	G:C→A:T	S37F
	10	94	GAT	AAT	G:C→A:T	D32N
50	5	122	ACC	ATC	G:C→A:T	T41I
	8	100	GGA	AGA	G:C→A:T	G34R
	12	94	GAT	AAT	G:C→A:T	D32N
	14	94	GAT	AAT	G:C→A:T	D32N
	16	110	TCT	TTT	G:C→A:T	S37F
	24	98	TCT	TAT	G:C→T:A	S33Y

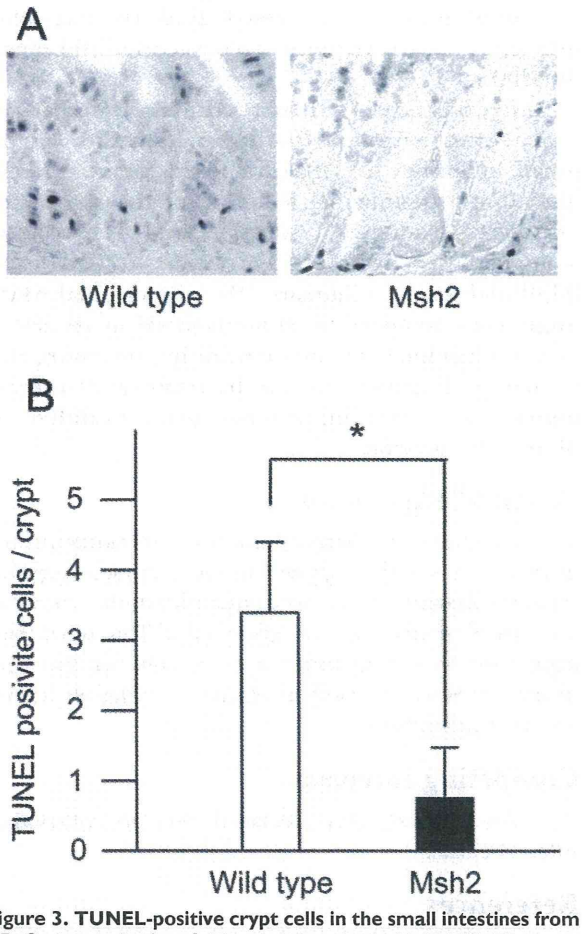

Figure 3. TUNEL-positive crypt cells in the small intestines from $KBrO_3$-treated mice. *A.* The sections stained with TUNEL. The crypts of small intestines from wild type (left) and *Msh2*-deficient (right) mice treated with $KBrO_3$. ***B.*** The number of TUNEL-positive cells in the crypts. The mean numbers of TUNEL-positive cells with standard deviations are indicated by white (wild type mice) and black (homozygous *Msh2*-deficient mice) bars. * $p<0.002$ (Student's *t*-test).

Analysis of cell death

MMR is involved in the signaling for cell death induced by genotoxic chemicals, such as alkylating agents (19-21). A previous study showed that ES cells carrying disrupted *Msh2* alleles displayed an increased survival following exposure to low-level ionizing radiation compared with wild type ES cells (26). The increased survival could be attributed to a failure of the cells to efficiently execute apoptosis in response to oxidative DNA damage induced by radiation exposure. These findings suggested that MMR is involved in the induction of apoptosis caused by oxidative DNA damage. It has been shown that intestinal cancer originates in the stem cells resided in the bottom of intestinal crypts (37). Thus, in the present study, we analyzed the cell death in the crypts of small intestines from wild type and *Msh2*-deficient mice treated with $KBrO_3$ using a TUNEL method. A few TUNEL-positive cells were detected in the crypts of wild type mice, but not in those of *Msh2*-deficient mice (Figure 3A). We counted the TUNEL-positive cells in more than 100 crypts from each genotype of mice. The average numbers of crypts per mouse were as follows: wild type, 21.2 (min 14, max 31) and *Msh2*-deficient, 21.6 (min 17, max 30). We found that 3.36 ± 0.96 (mean ± SD) TUNEL-positive cells per crypt were present in wild type mice, while 0.80 ± 0.46 (mean ± SD) TUNEL-positive cell per crypt were present in *Msh2*-deficient mice (Figure 3B). This difference was statistically significant ($p< 0.002$; *t*-test).

Discussion

In the present study, we performed $KBrO_3$-induced tumorigenesis experiments using *Msh2*-deficient mice to examine the involvement of mismatch repair (MMR) in the suppression of oxidative stress-induced tumorigenesis. The oral administration of $KBrO_3$ at a dose of 0.2% in drinking water dramatically increased the formation of intestinal tumors in *Msh2*-deficient mice compared to untreated *Msh2*-deficient mice and treated wild type mice. Thus, we concluded that MMR plays a significant role preventing the intestinal tumorigenesis induced by oxidative stress in mice.

Several lines of evidence suggest that oxidative stress could be generated in the intestines of animals under physiological conditions. For example, it was reported that the incidence of G:C to T:A transversions increases significantly in the intestines of older mice compared with younger mice (38). Because G:C to T:A transversions are mainly caused by 8-oxoG, a major oxidative DNA damage, these observations indicate that the mutations caused by oxidative DNA damage would tend to accumulate in the intestines during the course of aging. Consistent with this notion, defects in MUTYH, the human DNA glycosylase suppressing 8-oxoG-induced mutagenesis, lead to a susceptibility to colorectal cancers with excess G:C to T:A transversions in humans (39). Furthermore, *Mutyh*-deficient mice also show susceptibility to spontaneous and $KBrO_3$-induced intestinal adenoma/carcinoma (34). Therefore, based on these previous observations and our present results, it is likely that on a MMR-defective genetic background, oxidative stress generated in the intestine may enhance tumor development, thus leading to HNPCC in humans.

The mutation analyses of the tumor-related gene, *Ctnnb1*, revealed that more than 30% of the tumors that developed in $KBrO_3$-treated *Msh2*-deficient mice had somatic mutations in the coding region for GSK3β phosphorylation sites. All the mutations detected